

# Thermoplastic hardened Cu–Ni–Si–Ag alloy

Beata KRUPIŃSKA<sup>1</sup> <sup>\*</sup>, Robert CHULIST<sup>2</sup>, Marcin KONDRACKI<sup>3</sup>, and Krzysztof LABISZ<sup>4</sup>

<sup>1</sup> Silesian University of Technology, Faculty of Mechanical Engineering, Department of Engineering Materials and Biomaterials, Konarskiego 18a, 44-100 Gliwice, Poland

<sup>2</sup> Institute of Metallurgy and Materials Science of Polish Academy of Sciences Reymonta 25, 30-059 Krakow, Poland

<sup>3</sup> Silesian University of Technology, Faculty of Mechanical Engineering, Department of Foundry Engineering, Konarskiego 18a, 44-100 Gliwice, Poland

<sup>4</sup> Silesian University of Technology, Faculty of Transport and Aviation Engineering, Department of Railway Transport, Konarskiego 18a, 44-100 Gliwice, Poland

**Abstract.** The paper aims to investigate the influence of silver addition on the microstructure of CuNi<sub>2</sub>Si<sub>1</sub> alloys. The investigated copper alloy was cast and then supersaturated, plastically deformed on the Gleeble 3800 simulator and finally aged. Structural changes were examined using optical microscopy, scanning electron microscopy (SEM) and transmission electron microscopy (TEM). Orientation mapping was completed with FEI Quanta 3D field emission gun scanning electron microscope (SEM) equipped with TSL electron backscattered diffraction (EBSD) system. The effect of structural and microstructural changes on hardness and conductivity was also investigated. Based on the mechanical tests it was found that the mechanical properties and conductivity are improved due to heat and plastic treatment. It was also found that the precipitation hardening raises the hardness to the level of 40% whilst an increase in conductivity by 20% is observed.

**Key words:** CuNi<sub>2</sub>Si<sub>1</sub> alloys; modification; thermoplastic treatment; structure.

## 1. INTRODUCTION

Contemporary materials engineering responds to technological progress and aims to develop alloys with good mechanical properties and high conductivity. By applying heat and plastic treatment, we can control these properties for some groups of materials.

One of the groups of such materials that are of great interest all over the world is copper alloys. Examples of research on the modification and processing of copper alloys can be seen in Japan [1–3], China [4,5], India [6–9], the USA [10–12], and the EU [13–21].

While analyzing individual groups of copper alloys, beryllium copper is distinguished by the best strength properties and, at the same time, high electrical conductivity as well as corrosion and abrasion resistance [21]. Unfortunately, copper alloys with the addition of beryllium are highly toxic. Comparatively, cadmium copper is also toxic; however, it is used for the production of, for example, electric traction cables. Nevertheless, the use of these materials is less recommended. Therefore, intensive research is carried out on copper alloys, in particular on Cu–Ni–Si systems. Their electrical and mechanical properties are similar and comparable to copper-beryllium alloys. These alloys are also used in the aviation and electronics industries [15, 21–26].

The strength and hardness of the Cu–Ni–Si alloy can be considerably increased by the precipitation of the  $\delta$ -Ni<sub>2</sub>Si phase.

On the other hand, Ag dissolves in the matrix and enables also precipitation strengthening. The hardening in the alloy tends to reduce the electrical conductivity of the Cu alloys because distortion of the lattice increases the electron scattering [27–29]. The addition of Ag does not cause a significant decrease in electrical conductivity [31, 32].

Therefore, the subject of interest of many research centers around the world is the modification of CuNi<sub>2</sub>Si<sub>1</sub> alloys, mainly by heat and plastic treatment, but also by modification of chemical composition with chromium, silver, and rhenium [16–20]. Large plastic deformation improves the mechanical properties of the CuNi<sub>2</sub>Si<sub>1</sub> alloy; however, the resistivity of the alloy increases due to a large number of dislocations. This in turn lowers the electrical conductivity. By using heat treatment (solution heat treatment and aging), it is possible to influence the value of the conductivity to some extent [14, 21]. On the other hand, using the rhenium modification, we obtain very good mechanical properties and an optimal value of conductivity compared to the properties of CuNi<sub>2</sub>Si<sub>1</sub> alloys [14–16, 22]. Additionally, by applying silver modification, good mechanical properties and an increase in the conductivity value compared to CuNi<sub>2</sub>Si<sub>1</sub> alloys can be obtained [20, 31].

In this context, the given studies provide valuable information on the effect of Ag addition on the hardening of heat-treated and plastically deformed Cu–Ni–Si alloys. The study shows the effect of silver addition with a mass concentration of 0.8% on the microstructure of CuNi<sub>2</sub>Si alloys. Overall, the research is carried out in order to optimize the silver content and heat treatment parameters.

\*e-mail: [beata.krupinska@polsl.pl](mailto:beata.krupinska@polsl.pl)

Manuscript submitted 2022-10-14, revised 2023-01-30, initially accepted for publication 2023-02-27, published in April 2023.

## 2. MATERIALS AND METHODS

A silver-modified Cu–Ni–Si alloy with the chemical composition given in Table 1 was used for testing. Ingots were cast into thick-walled cylindrical cast iron molds. The alloy was prepared with the use of an induction furnace. Pure ingredients were introduced into the heated crucible (600°C) and melted under a protective argon atmosphere. Argon was also fed to the stream during casting. The metal mold was preheated and the temperature during casting was 1150°C.

**Table 1**

Chemical composition of the investigated copper alloys

Alloys	Elements as compounds of the modelled Cu casts, mass%			
	Ni	Si	Ag	Cu
Cu–Ni–Si	2	1	–	balance
Cu–Ni–Si–Ag	2	1	0.8	balance

The heat treatment of CuNi2Si1Ag0.8 alloys was performed at the temperature of 770°C; solution heat treatment and subsequent ageing were performed at the temperature of 500°C. After solution heat treatment, a cold plastic deformation with a 50% degree of thickness reduction was performed. The parameters of thermo-mechanical treatment are given in Table 2. Parameters of the CuNi2Si1 alloys were selected on the basis of the literature data [13–15]. On the other hand, CuNi2Si1Ag0.8 was determined as part of our own experiments.

Heat treatment and cold plastic deformation were carried out with the application of a thermo-mechanical simulator

**Table 2**

Thermo-mechanical treatment parameters

CuNi2Si1			
	Solution heat treatment	Plastic deformation	Ageing
Processing temperature	950°C	room temperature	500°C
Time	1 h	–	1 h
Cooling speed	20 s	–	–
Deformation rate	–	100 s <sup>-1</sup>	–
CuNi2Si1Ag0.8			
	Solution heat treatment	Plastic deformation	Ageing
Processing temperature	770°C	room temperature	500°C
Time	1 h	–	1 h
Cooling speed	20 s	–	–
Deformation rate	–	100 s <sup>-1</sup>	–

from DSI (Dynamic System Inc.) Gleeble 3800. The additional equipment of the Gleeble 3800 simulator was a direct resistance heating system which assures the maintenance of the desired temperature with an accuracy of  $\pm 1^\circ\text{C}$ . The use of the Gleeble simulator allowed us to perform heat treatment at a strictly defined temperature. It minimized errors that may have occurred during heating, annealing and direct cooling with a jet of water under pressure or compressed. A set of graphite and tantalum layers with a thickness of 0.1 mm was used to connect the surfaces of the sample. Additionally, the anvils were coated with nickel-based grease to protect the samples from joining the tungsten carbide anvil. It improved the contact between the surfaces (it is of high importance in the case of resistance heating carried out in the simulator and consisting of the flow of current through the test sample), friction between the joint surface of the test sample and the surface of the tungsten carbide anvil.

The following tests were performed:

- Microstructure analysis of the alloy was performed using both a ZEISS optical microscope and image analysis software. During preparation for the observation of the microstructure samples were subjected to grinding and mechanical polishing, then electropolishing and etching in an electrochemical reagent (D2) or in a reagent composed of iron chloride, hydrochloric acid and ethyl alcohol.
- The microstructure and chemical composition were examined by the EDS microanalysis method using: scanning electron microscopes Zeiss Supra 25 and MEF4A as well as on the Leco GDS 500A spectrometer.
- TEM studies were carried out with the application of the S/TEM Titan 80–300 microscope fitted with a Cetcor Cs probe corrector and an EDS and EELS spectrometer for chemical composition analysis. Crystal Maker and Single Crystal software (CrystalMaker Software Limited, version 10.4.1, Oxfordshire, Great Britain) were utilized to simulate the crystal structure and diffraction patterns.
- The preparations for examination in the high-performance transmission microscope were prepared in the SEM/Xe-PFIB FEI Helios PFIB Microscope. The lamellas were prepared by applying a protective layer of platinum and then cut with a focused beam of xenon plasma ions (Xe-PFIB). The samples were prepared by applying a protective layer of platinum and then cut with a focused xenon plasma ion beam (Xe-PFIB). Orientation mapping was organized with the use of the FEI Quanta 3D field emission gun scanning electron microscope (SEM); its additional equipment was TSL electron backscattered diffraction (EBSD) system.
- Low-load hardness test was performed with a Vickers Future-Tech hardness tester (FM-ARS 9000) with a load of 1000 gf for 10 s.
- The electrical conductivity was measured with a Sigmatest Foerster 2.069 device. Measurements were carried out at ambient temperature with an operating frequency of 60 kHz. Sample testing was preceded by the calibration of the device on a set of two standards with electrical conductivity values of 4.4 MS/m (8% IACS) and 58 MS/m (100% IACS).

### 3. RESULTS AND DISCUSSION

The microstructure of the CuNi2Si1 alloy with the addition of Ag after solidification from the temperature of 1091°C consists of dendrites of the  $\alpha$  Ni<sub>2</sub>Si phase and Ag phases in the interdendritic spaces (Fig. 1).

After solution heat treatment and plastic deformation, numerous deformation bands (Figs. 2a, 2b) and the fragmented Ni<sub>2</sub>Si phase are visible. As can be seen in Figs. 2c, 3 and 4, silver is dissolved in the matrix. The chemical composition analysis is shown in Figs. 2d, 4 and 5.

During aging at the temperature of 500°C, the silver precipitates in the matrix. The structure consists of recrystallized grains of the  $\alpha$  phase, Ni<sub>2</sub>Si phase and Ag precipitation. Uniform dissolution occurred after the analyzed CuNi2Si1Ag0.8 alloy was supersaturated silver in the ground mass. The Ni<sub>2</sub>Si phases are long phases with different spatial orientations – it is observed in the EDS analysis, the size of the precipitates is about 500–1000 nm (Figs. 2–6).

The solution heat treatment took place on the Gleeble 3800 simulator, where the sample was compressed with minimal

force during treatment. This minimal force was used in order to promote silver diffusion towards the grain boundary.

The solution heat treatment temperature during compression cannot exceed the Cu–Ag eutectic temperature, i.e. 770°C, because the eutectic regions may transform to a semi-solid state by partial melting causing material flows (Fig. 2).

**Table 3**

Results of the EDS spectrum analysis for the areas from Fig. 1c (wt.%)

Element	Point #1	Point #2
Si	–	11.53
Ag	83.36	07.48
Ni	–	34.24
Cu	16.64	46.76

Based on electron diffraction (Fig. 5), NiSi precipitates were identified as Ni<sub>2</sub>Si (hexagonal crystal; space group: P 63 2 2; reference code: 96-152-3552) [33].

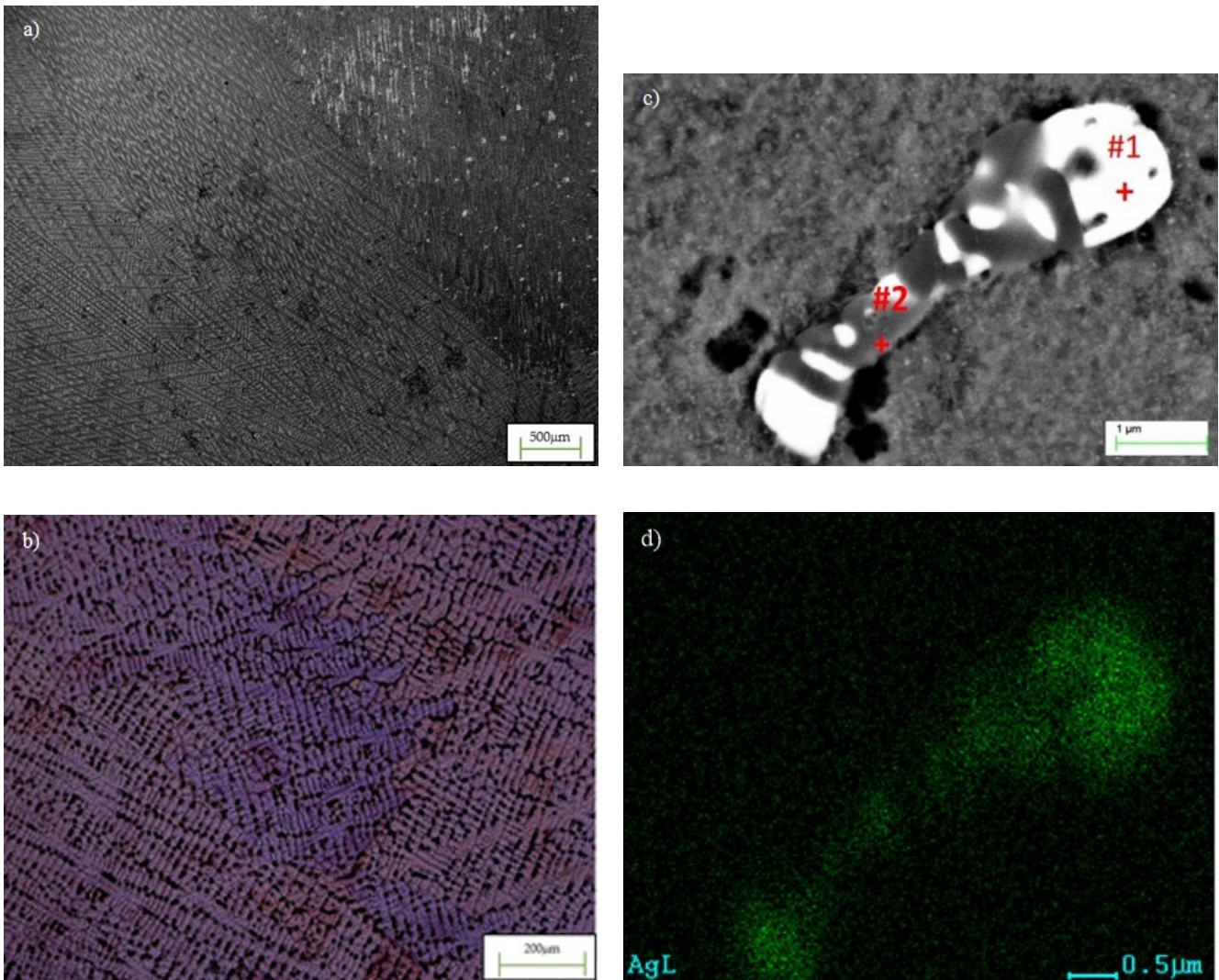


**Fig. 1.** (a)–(c) Structure of CuNi2Si1Ag0.8 alloy, initial state (d); mapping structure CuNi2Si1Ag0.8



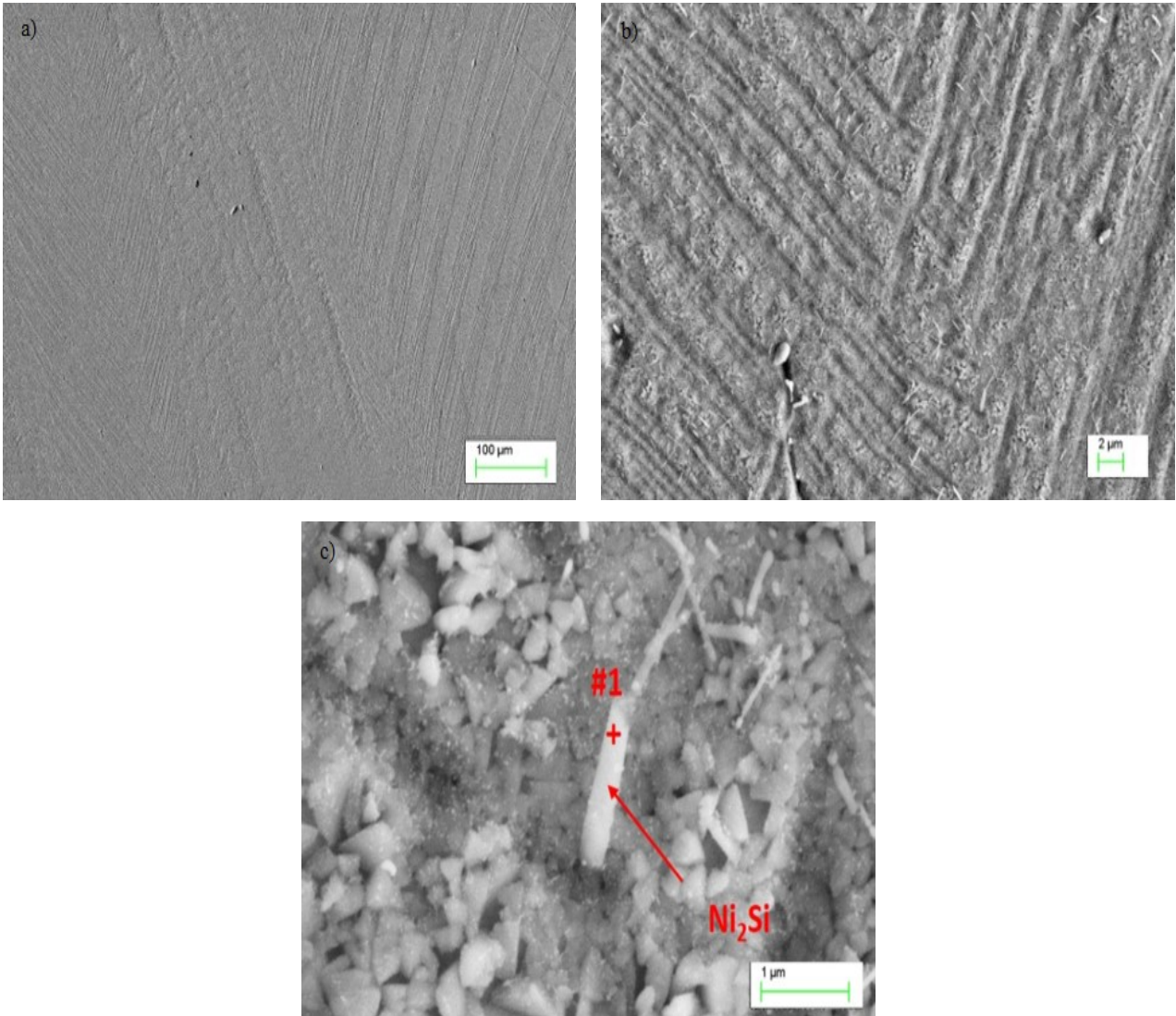


**Fig. 2.** (a)–(c) Structure of CuNi<sub>2</sub>Si<sub>1</sub>Ag<sub>0.8</sub> alloy: solution heat treatment at 770°C; time 1 h, cooling in water (Ar); cold plastic deformation 50%; ageing 500°C 1 h

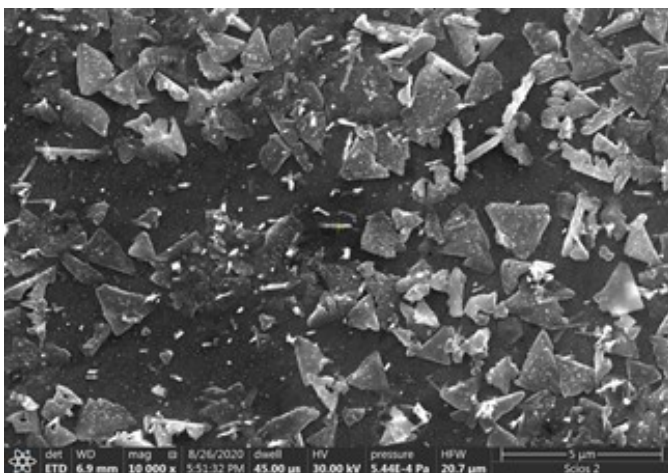


**Fig. 3.** Structure of CuNi<sub>2</sub>Si<sub>1</sub>Ag<sub>0.8</sub> alloy, solution heat treatment at 770°C; time 1 h, cooling in water (Ar); cold plastic deformation 50%; ageing 500°C 1 h

**Table 4**

Results of the EDS spectrum analysis for the areas from Fig. 2c (wt.%)

Element	Point #1
Si	04.97
Ag	02.61
Ni	18.10
Cu	74.32

Additionally, Ag precipitates were observed in the form of fibers perpendicular to the direction of deformation located mostly on the grain boundary of the  $\alpha$  phase.

Analysis of the phase and crystallographic orientation of grains (EBSD) by scanning electron microscopy along with a map of the distribution of crystallographic orientations and texture is presented in Figs. 7 and 8.

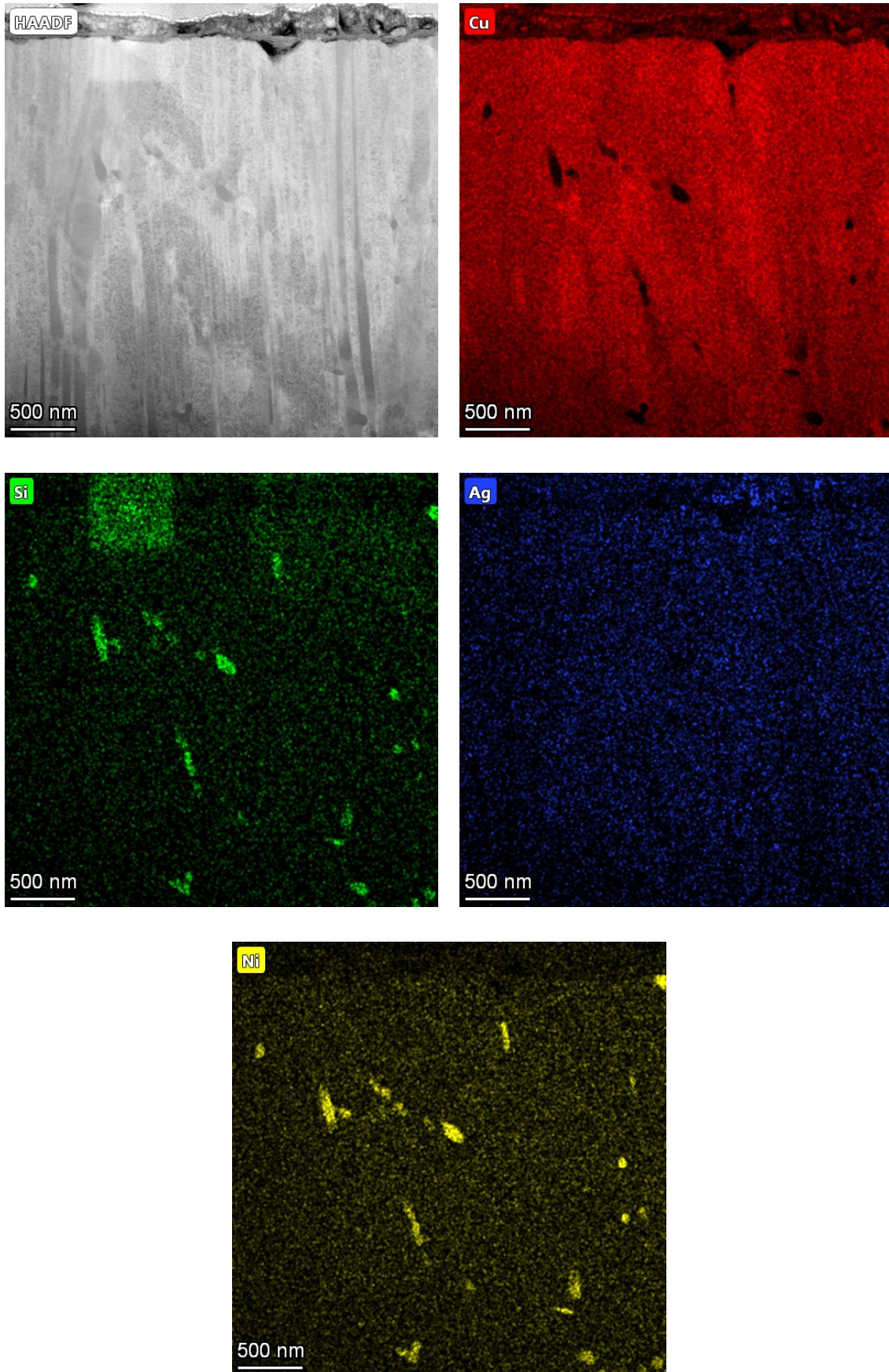


**Fig. 4.** Structure of CuNi<sub>2</sub>Si<sub>1</sub>Ag<sub>0.8</sub> alloy: solution heat treatment at 770°C; time 1 h, cooling in water (Ar); cold plastic deformation 50%; ageing 500°C 1 h



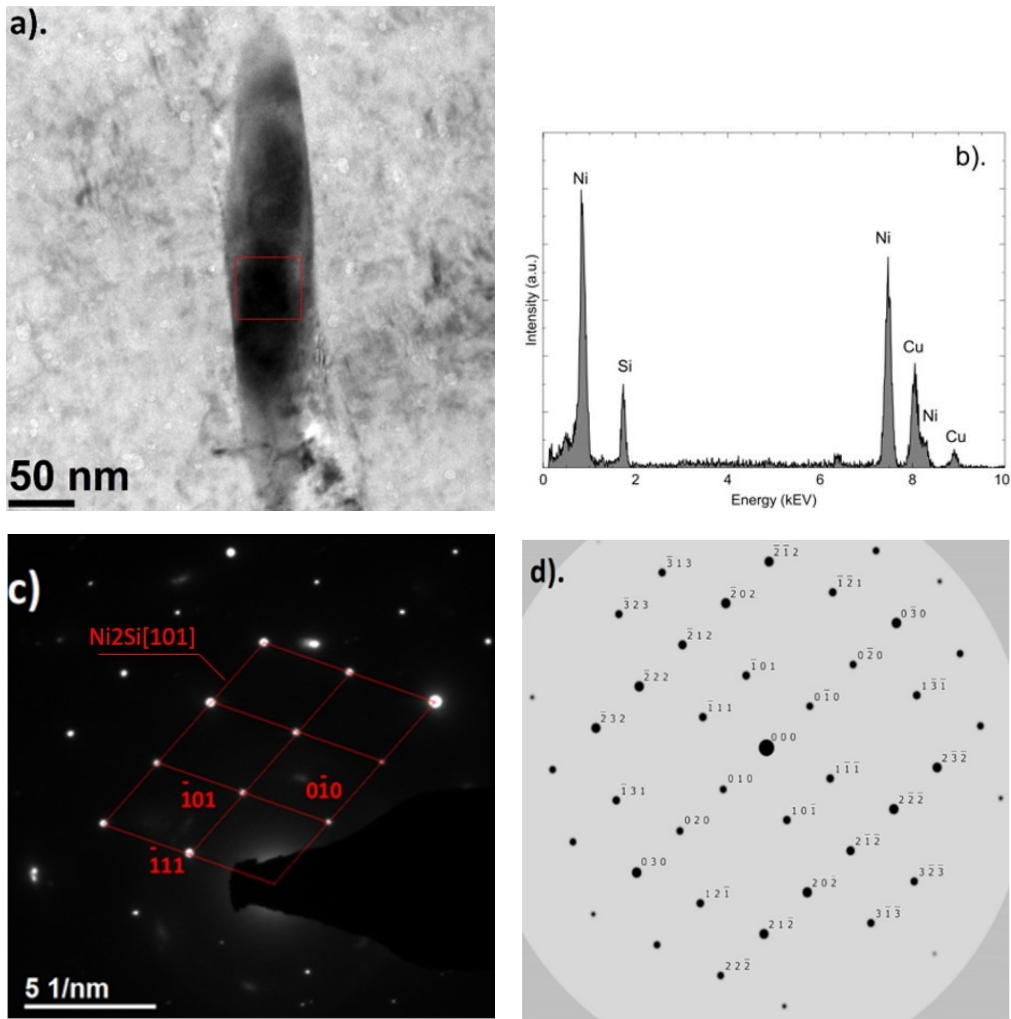


**Fig. 5.** Ni<sub>2</sub>S particle embedded in the substrate material: a) TEM image; b) EDS spectrum obtained for the area indicated at a); c) SAED electron diffraction of Ni<sub>2</sub>Si on the zone axis and d) computer simulation of the electron diffraction solution of the of Ni<sub>2</sub>S in the [101]

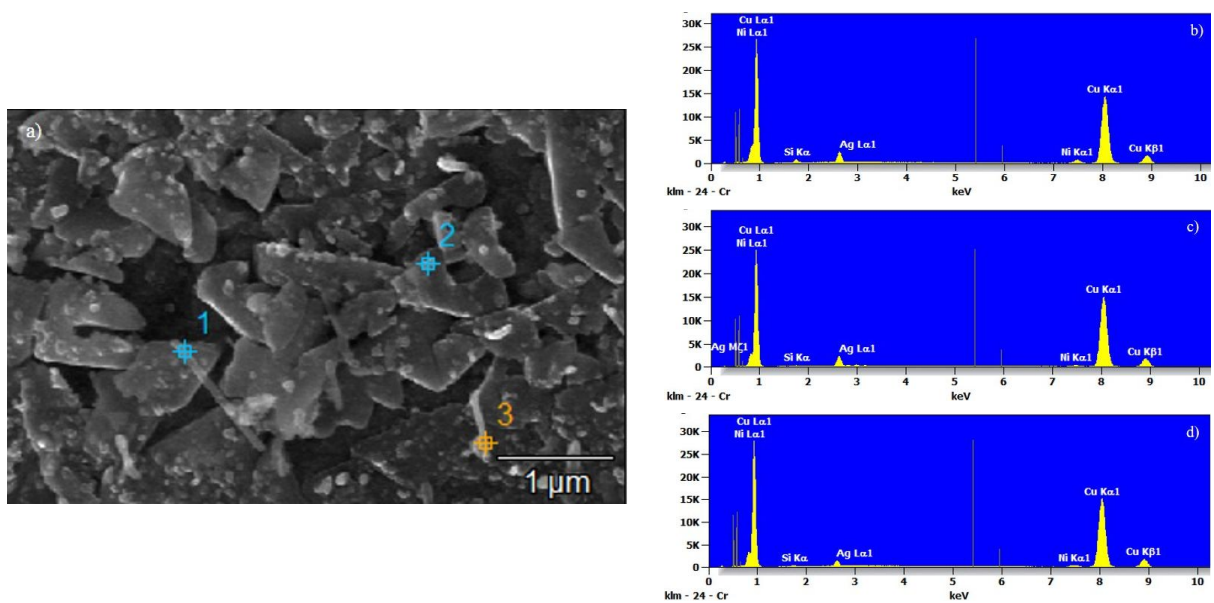


**Fig. 6.** a) Structure of CuNi<sub>2</sub>Si<sub>1</sub>Ag<sub>0.8</sub> alloy: solution heat treatment at 770°C; time 1 h, cooling in water (Ar); cold plastic deformation 50%; ageing 500°C 1 h; b) analysis of point 1 made with energy-dispersive X-ray spectroscopy; c) analysis of point 2 made with energy-dispersive X-ray spectroscopy; d) analysis of point 3 made with energy-dispersive X-ray spectroscopy

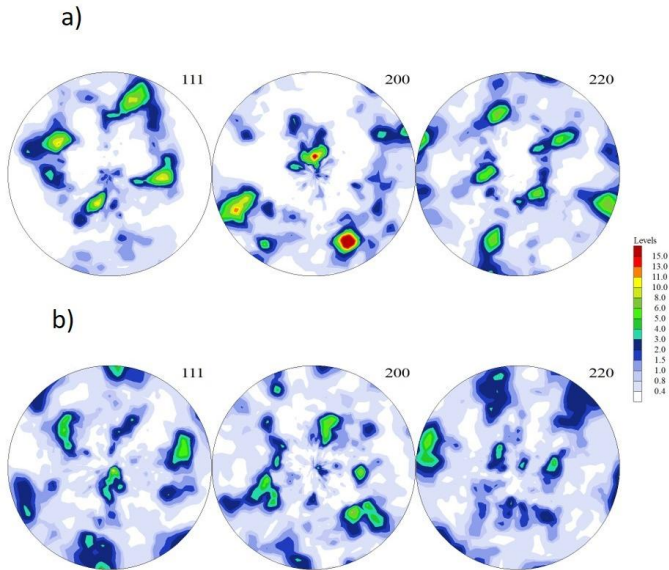


**Fig. 7.** a) (111), (200), (220) pole figures of CuNi<sub>2</sub>Si<sub>1</sub>Ag<sub>0.8</sub> alloy in the cast state; b) (111), (200), (220) pole figures of CuNi<sub>2</sub>Si<sub>1</sub>Ag<sub>0.8</sub> alloy: solution heat treatment at 770°C; time 1 h, cooling in water (Ar); cold plastic deformation 50%; ageing 500°C 1 h. Compression direction on the top

The orientation map shown in the figure presents the microstructure with deformed grains after compression with a 50% deformation degree in the Gleeble 3800 simulator. Moreover, the grains have a texture with (111) plane parallel to the compression direction.

The cold compaction produces deformed microstructure with deformation bands visible also after aging at the temperature of 500°C. The deformed and aged alloy is additionally reinforced by the precipitation of Ni<sub>2</sub>Si phases. This process is stimulated by plastic deformation providing preferential sites for nucleation.

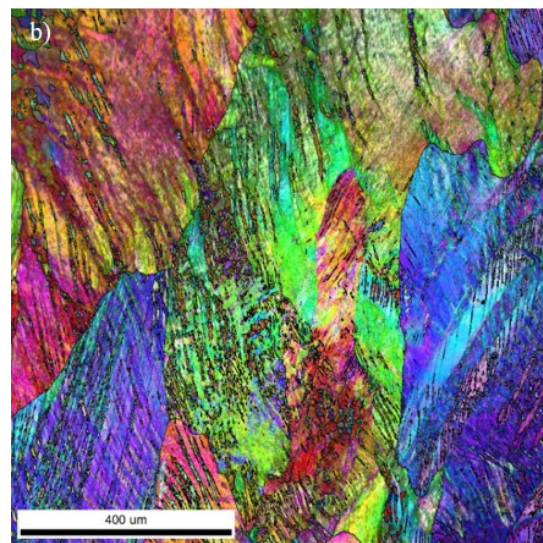
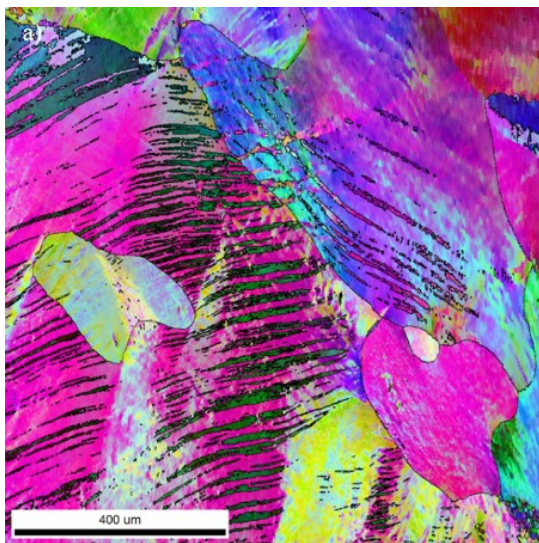


**Fig. 8.** a) Electron backscatter diffraction (EBSD) images of the structure of CuNi<sub>2</sub>Si<sub>1</sub>Ag<sub>0.8</sub> alloy in the cast state; b) Electron backscatter diffraction (EBSD) images structure of CuNi<sub>2</sub>Si<sub>1</sub>Ag<sub>0.8</sub> alloy: solution heat treatment at 770°C; time 1 h, cooling in water (Ar); cold plastic deformation 50%; ageing 500°C 1 h

As a result of the precipitation process of Ni<sub>2</sub>Si, but also the precipitation of fine Ag phases, the hardness of the CuNi<sub>2</sub>Si<sub>1</sub>Ag<sub>0.8</sub> alloy after treatment is 195 HV, which is approximately 40% higher than for the CuNi<sub>2</sub>Si<sub>1</sub> alloy (Fig. 8). After the heat and plastic treatment, the conductivity in the CuNi<sub>2</sub>Si<sub>1</sub>Ag<sub>0.8</sub> alloy also increases by about 20% compared to the alloy without the addition of Ag (Fig. 9). The basic conductivity of the CuNi<sub>2</sub>Si<sub>1</sub>Ag<sub>0.8</sub> alloy is slightly higher than the one of the CuNi<sub>2</sub>Si<sub>1</sub> alloy.

The hardness measurements at low load were made at 20 test points on 4 samples. The changes in hardness at low load force and conductivity are shown in Fig. 9. One can observe that the alloy with Ag addition after heat treatment and plastic deformation is characterized by a higher hardness of about 45 HV and higher conductivity of about 4 Ms/m.

In the further part of the research on the alloys, they will focus on the influence of heat treatment time and temperature, plastic working in the form of rolling and drawing, and Ag content on the mechanical properties and conductivity.

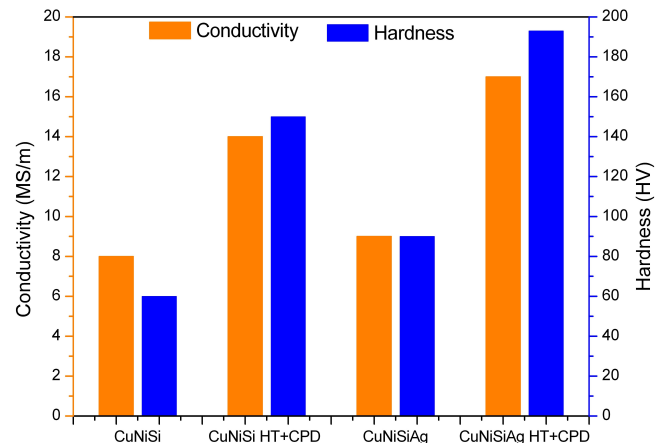


**Fig. 9.** Hardness and conductivity of CuNi<sub>2</sub>Si<sub>1</sub> and CuNi<sub>2</sub>Si<sub>10</sub>Ag<sub>0.8</sub> alloys (HT + CPD – after heat treatment plus cold plastic deformation)



#### 4. CONCLUSIONS

The investigation of CuNi2Si1 alloys modified with Ag at the level of 0.8% mass showed that:

1. The addition of silver combined with the thermo-plastic treatment on the Gleeble simulator causes an increase in hardness by 40% (the hardness of the thermo-mechanically treated CuNi2Si1 alloy was 150 HV, after adding silver it is 193 HV).
2. The conductivity for the thermo-plastically treated Ag modified alloy is 18 Ms/m which is about 20% higher than for the non-modified alloy.
3. Aging of the supersaturated and previously deformed CuNi2Si1Ag0.8 alloy causes precipitation of Ni<sub>2</sub>Si phases.
4. Modification of the chemical composition with silver at a concentration of 0.8% mass causes an increase in hardness and an increase in conductivity.
5. The Ni<sub>2</sub>S precipitate particles confirmed by TEM analysis occur in a longitudinal needle-formed shape of a length of ca. 500 nm, improving the strengthening of the alloy due to similar size compared to the EBSD revealed grained/sub-grained microstructure.

#### REFERENCES

- [1] T.J. Konno, R. Nishio, S. Semboshi, T. Ohsuna, and E. Okunishi, "Aging behavior of Cu–Ti–Al alloy observed by transmission electron microscopy," *J. Mater. Sci.*, vol. 43, pp. 3761–3768, 2008.
- [2] S. Semboshi, T. Al-Kassab, R. Gemma, and R. Kirchheim, "Microstructural evolution of Cu–1 at% Ti alloy aged in a hydrogen atmosphere and its relation with the electrical conductivity," *Ultramicroscopy*, vol. 109, pp. 593–598, 2009.
- [3] S. Semboshi, T. Nishida, and H. Numakura, "Microstructure and mechanical properties of Cu–3% at. Ti alloy aged in a hydrogen atmosphere," *Mater. Sci. Eng. A-Struct.*, vol. 517, pp. 105–113, 2009.
- [4] D.P. Lu, J. Wang, W.J. Zeng, Y. Liu, L. Lu, and B.-D. Sun, "Study on high-strength and high conductivity Cu–Fe–P alloys," *Mater. Sci. Eng. A-Struct.*, vol. 421, pp. 254–259, 2006.
- [5] D. Zhao, Q.M. Dong, P. Liu, B.X. Kang, J.L. Huang, and Z.H. Jin, "Aging behavior of Cu–Ni–Si alloy," *Mater. Sci. Eng. A-Struct.*, vol. 361, pp. 93–99, 2003.
- [6] S. Nagarjuna and D.S. Sarma, "Effect of cobalt additions on the age hardening of Cu–4.5Ti alloy," *J. Mater. Sci.*, vol. 37, pp. 1929–1940, 2002.
- [7] R. Markandeya, S. Nagarjuna, and D.S. Sarma, "Precipitation Hardening of Cu–3Ti–1Cd Alloy," *J. Mater. Eng. Perform.*, vol. 16, pp. 640–646, 2007.
- [8] S. Thanga Kasi Rajan, A.N. Balaji, P. Narayanasamy and S.C. Vettivel, "Microstructural, electrical, thermal and tribological studies of copper fly ash composites through powder metallurgy," *Bull. Pol. Acad. Sci. Tech. Sci.*, vol. 66, no. 6, pp. 935–940, 2018, doi: [10.24425/bpas.2018.125941](https://doi.org/10.24425/bpas.2018.125941).
- [9] S. Nagarjuna, K. Balasubramanian, and D.S. Sarma, "Effect of Ti additions on the electrical resistivity of copper," *Mater. Sci. Eng.*, vol. 225, pp. 1118–1124, 1997.
- [10] T. Radetic, V. Radmilovic, and W.A. Soffa, "Electron microscopy observations of deformation twinning in a precipitation hardened copper-titanium alloy," *Scripta Mater.*, vol. 35, no. 12, pp. 1403–1409, 1996.
- [11] T. Radetic, V. Radmilovic, and W.A. Soffa, "Electron microscopy observations of twin-twin intersections in a particle hardened copper-titanium alloy," *Scripta Mater.*, vol. 40, no. 7, pp. 845–852, 1999.
- [12] D.E. Laughlin and A.W. Soffa, "Spinodal Structures, Metals Handbook, Ninth Edition: Metallography and Microstructures," *Am. Soc. Met.*, vol. 9, pp. 652–654, 1985.
- [13] J. Stobrawa and Z. Rdzawski, "The Structure of Coherent Chromium and Iron Precipitates in Aged Copper Alloys," *Works Inst. Non-Ferrous Met.*, vol. 9, pp. 221–224, 1980.
- [14] J. Stobrawa, Z. Rdzawski, W. Gluchowski, and W. Malec, "Microstructure and properties of CuNi2Si1 alloy processed by continuous RCS method," *J. Achiev. Mater. Manuf. Eng.*, vol. 37, pp. 466–479, 2009.
- [15] Z. Rdzawski and J. Stobrawa, "Thermomechanical processing of CuNiSiCrMg alloy," *Mater. Sci. Technol.* Vol. 9, pp. 142–149, 1993.
- [16] Z. Rdzawski, "Copper Alloy"; Silesian University of Technology: Gliwice, Poland, 2009.
- [17] B. Krupińska and Z. Rdzawski, "Effect of Re addition on the crystallization, heat treatment and structure of the Cu–Ni–Si–Cr alloy," *J. Therm. Anal. Calorim.*, vol. 134, pp. 173–179, 2018, doi: [10.1007/s10973-018-7668-y](https://doi.org/10.1007/s10973-018-7668-y).
- [18] B. Krupińska, Z. Rdzawski, M. Krupiński, and W. Pakieła, "Precipitation Strengthening of Cu–Ni–Si Alloy," *Materials*, vol. 13, no. 5, p. 1182, 2020, doi: [10.3390/ma13051182](https://doi.org/10.3390/ma13051182).
- [19] T. Knych, P. Kwaśniewski, and I.A. Kawecki, "Impact of supersaturation conditions of CuNi2Si alloy on its mechanical and electrical properties after artificial aging," in *Proceedings of the 37th School of Materials Engineering*, Poland, 2009, pp. 135–138.
- [20] B. Krupińska, W. Borek, M. Krupiński, and T. Karoszka, "The Influence of Ag on the Microstructure and Properties of Cu–Ni–Si Alloys," *Materials*, vol. 15, no. 13, p. 3416, 2020, doi: [10.3390/ma13153416](https://doi.org/10.3390/ma13153416).
- [21] W. Gluchowski, Z. Rdzawski, J. Sobota, and J. Domagała-Dubieli, "Effect of the Combined Heat Treatment and Severe Plastic Deformation on the Microstructure of CuNiSi Alloy," *Arch. Metall. Mater.*, vol. 61, no. 2, pp. 1207–1214, 2016.
- [22] S. Tao, Z. Lu, H. Xie, H.J. Zhang, and X. Wei, "Effect of high contents of nickel and silicon on the microstructure and properties of Cu–Ni–Si alloys," *Mater. Res. Express*, vol. 9, p. 046516, 2022, doi: [10.1088/2053-1591/ac64ec](https://doi.org/10.1088/2053-1591/ac64ec).
- [23] S. Tao, Z. Lu, H. Xie, H. J. Zhang and X. Wei, "Effect of preparation method and heat treatment on microstructure and properties of Cu–Ni–Si alloy," *Mater. Lett.*, vol. 315, 2022, doi: [10.1016/j.matlet.2022.131790](https://doi.org/10.1016/j.matlet.2022.131790).
- [24] H. Fu, J. Li, and X. Yun, "Role of solidification texture on hot deformation behavior of a Cu–Ni–Si alloy with columnar grains," *Mater. Sci. Eng. A-Struct.*, vol. 824, p. 141862, 2021, doi: [10.1016/j.msea.2021.141862](https://doi.org/10.1016/j.msea.2021.141862).
- [25] *Copper & Copper Alloys, Composition & Properties*, Technical Note TN10, Copper Development Association Inc., 1986.
- [26] L. Jia *et al.*, "Microstructure evolution and reaction behavior of Cu–Ni–Si powder system under solid-state sintering," *Mater. Chem. Phys.*, vol. 271, p. 124942, 2021, doi: [10.1016/j.matchemphys.2021.124942](https://doi.org/10.1016/j.matchemphys.2021.124942).
- [27] H. Wei, Y. Chen, Y. Zhao, W. Yu, L. Su, and D. Tang, "Correlation mechanism of grain orientation/microstructure and mechanical properties of Cu?Ni?Si?Co alloy," *Mater. Sci. Eng. A-Struct.*, vol. 814, p. 141239, 2021, doi: [10.1016/j.msea.2021.141239](https://doi.org/10.1016/j.msea.2021.141239).



- [28] C. Watanabe, S. Takeshita, and R. Monzen, “Effects of Small Addition of Ti on Strength and Microstructure of a Cu–Ni–Si Alloy,” *Metall. Mater. Trans. A*, vol. 46, pp. 2469–75, 2015.
- [29] I.V. Alexandrov, M.V. Zhilina, and J.T. Bonarski, “Formation of texture inhomogeneity in severely plastically deformed Copper,” *Bull. Pol. Acad. Sci. Tech. Sci.*, vol. 54, no. 2, pp. 199–208, 2006.
- [30] R.A.G. Silva, A. Paganotti, A.T. Adorno, C.M.A. Santos, and T.M. Carvalho, “Precipitation hardening in the Cu–11 wt.%Al–10 wt.%Mn alloy with Ag addition,” *J. Alloy. Compd.*, vol. 643(S1), pp. S178–S181, 2015, doi: [10.1016/j.jallcom.2014.12.208](https://doi.org/10.1016/j.jallcom.2014.12.208).
- [31] Y. Liu, S. Shao, K.M. Liu, X.J. Yang, and D.P. Lu, “Microstructure refinement mechanism of Cu–7Cr in situ composites with trace Ag,” *Mater. Sci. Eng. A*, 2012, 531, 141–146.
- [32] Y. Zhang *et al.*, “Deformation Behavior And Microstructure Evolution Of The Cu–2Ni–0.5Si–0.15Ag Alloy During Hot Compression,” *Metall. Mater. Trans. A*, vol. 46, pp. 5871–5876, 2015, doi: [10.1007/s11661-015-3150-7](https://doi.org/10.1007/s11661-015-3150-7).
- [33] M. Ellner, M.K. Bhargava, S. Heinrich, and K. Schubert, “Einige strukturelle untersuchungen in der mischung NiSi<sub>N</sub>,” *J. Less-Common Met.*, vol. 66, pp. 163–173, 1979, doi: [10.1016/0022-5088\(79\)90226-1](https://doi.org/10.1016/0022-5088(79)90226-1).